Journal of Petroleum Science and Engineering 152 (2017) 317–329

Contents lists available at ScienceDirect

Journal of Petroleum Science and Engineering

journal homepage: www.elsevier.com/locate/petrol

New type plugging particle system with high temperature & high salinity resistance

Fenglan Zhao[a,*], Zihao Li[a], Jieheng Wu[b], Jirui Hou[a], Shiyuan Qu[c]

[a] Enhanced Oil Recovery Institute, China University of Petroleum (Beijing), Beijing 102249, China
[b] Changqing Division, CNPC Logging, Xi'an 710077, China
[c] College of Petroleum Engineering, China University of Petroleum (Beijing), Beijing 102249, China

ARTICLE INFO

Keywords:
Particle
Plugging properties
High temperature & salinity
Visual experiments
Force analysis

ABSTRACT

A new-type plugging coated particle system was investigated which is applied in high temperature & salinity reservoir, the temperature up to 300 ℃ and salinity up to 250,000 mg/L. To analyze these factors, based on adhesion feature of the particle, a series of experiments were performed to investigate properties of particle and its suspension system, including dynamic plugging experiments, etc. The results showed that the particles can adhere together under certain temperature up to 140 ℃. Moreover, the particle suspension, including HPG system and foam system, were screened based on suspending time. In addition, we selected four parameters, including salinity, injection rate, permeability and mass fraction, to measure plugging ability of system. Meanwhile, the visual microscopic models and glass sand-pack models were designed to observe directly particle flow in the porous media. Finally, the force analysis of particles at some special locations in the models was simulated by COMSOL Multiphysics. Experimental results confirmed the essential characters of new-type particle and indicate that this plugging system had excellent plugging performance in high temperature & salinity environment. The particle migration had strong correlation with permeability and the particle had impacted on the original structure of mineral. The process of packing was accelerated and repeated. Besides, keeping the particle single and improving material strength would promote plugging effects. The evaluation and mechanism research of new type plugging particle could provide guidance for plugging agent selection in high temperature and field development project designing.

1. Introduction

Global consumption of oil and natural gas energy has rapidly increased during the past few years. To meet the enormous demands of energy, the reservoir with high temperature and salinity, which used to be regarded as the back-up resources, have been developed in large scales (Zhao et al., 2005; Sharma et al., 2013; Galindo et al., 2015; Quadri et al., 2015;). Meanwhile, as one of the priority means in development, profile control and plugging technique could enhance developing effect to a large extent (Jones et al., 1992; Ojukwu et al., 2005; Xiong et al., 2007; Hernando et al., 2016;). The research on this subject include matched plugging agent and the former studies about this topic usually focused on polymer gel (Bryant et al., 1996; Hild et al., 1999; Liu et al., 2006), inorganic gel (Fragachan et al., 1996; Lakatos et al., 1996) and performed-particle-gel (Bai et al., 2011; Cui et al., 2011; Elsharafi et al., 2015), etc. However, due to high temperature and high salinity, traditional chemical plugging agents can't satisfy the conditions in these reservoirs.

This new type of particle belongs to inorganic particle, which have wide range of sources and low cost (Zhao et al., 2015). For this particle, the plugging mechanism is based on bridging plugging theory. And the bridging plugging theory means the rigid plugging materials are set up in the leakage pores like bridges and then the lower-level materials are continued to fill voids or bridging in smaller pores, so the permeability can be decreased and the pressure will be tolerated by these plugging materials (Zheng and Zhang, 2012). The relationships between plugging materials and leakage pores about size has been investigated by former relevant studies (Abrams, 1977; Khatib and Vitthal, 1991; Luo and Luo, 1992; Li et al., 1995; Cui et al., 2000), Civan (2007) reported that the impact of pore geometry can be predicted in a straight forward way by using an aspect ratio (β=pore throat to particle diameter length ratio) correlation: if β≤7, then bridging can occur. Besides, Civan and Vinh (2005) and Tran et al. (2009, 2010) observed an exponential correlation for the dynamic permeability as a function of time with exponents and coefficients depending on several variables including cement exclusion parameter, particle volume fraction and pore-to-

* Corresponding author.
E-mail address: zhaoflan123@163.com (F. Zhao).

http://dx.doi.org/10.1016/j.petrol.2017.03.024
Received 28 September 2016; Received in revised form 22 December 2016; Accepted 8 March 2017
Available online 10 March 2017
0920-4105/

particle diameter. We designed the approximate size range based on the studies above. Furthermore, the particle is composed of core and coat. The coat, which is made by modified epoxide resin with different melting points, will melt and adhere with other particles or pore wall to enhance plugging intensity. Because of the melting points, the coat with different types of particles can melt under different temperatures to satisfy various temperature conditions in reservoirs. Comparing with the PPG (Bai, 2003) which was one of the most successful plugging agents, the plugging mechanism of this plugging particle was different and had the potential to be suitable to the high temperature environment which PPG could not adapt.

To investigate more about this particle, we conducted a series of experiments, ranging from particle essential characters, suspension screening to dynamic plugging experiments, simulation analysis. The experiments showed the particles could splice each other steadily under high pressure or temperature and suspend in the HPG system or foam system. Moreover, we summed up results of 26 groups of dynamic plugging experiments and found that permeability was the most crucial factor which defined plugging effect of particle, other factors such as injection rate, injection volume, and particle concentration would also impact the final effect. By observing the migration of particles in and glass sand-pack models, we confirmed that the degree of particle's deep migration was impacted by permeability and particles might change original grains location. And by the visual microscopic models, the results showed that the packing of particles was repeated and accelerated. And the simulation analysis by the COMSOL Multiphysics presented keeping particle single was important and improving particle intensity would be benefit for plugging effects.

2. Methodology

2.1. Materials

Due to the difference of diameter and coat, this particle could be divided into several types. We selected two types of them to conduct the following experiments and these particles were separately named 1-S and 2-S. The particles used in the experiment were 1-S or 2-S particles (Fig. 1), their coats were both modified epoxide resin. The average diameters of particle 1-S and 2-S were respectively 174 μm and 92 μm. The suspensions were HPG (guar hydroxypropyl trimonium chloride) or foam system with certain formula.

2.2. Equipment

Four types of experiments were conducted in total, so the experimental equipment were also various. To test the particle essential characters, equipment like microscope, scale, high-temperature and high-pressure reactors, oven was utilized. And for screening the suspension, we prepared measuring cylinder, balance, timer, etc. Besides, the sand-packed pipe, oven, pressure sensor, computer, constant-flux pump was performed to the dynamic plugging experiment. Finally, except microscope, computer, camera, timer, constant-flux pump, etc. the equipment in visual model experiment also included Glass Sand-Pack Models and Visual Microscopic Models which we designed.

A. Particle 1-S B. Particle 2-S C. Particle Structure

Fig. 1. Particles 1-S and 2-S.

2.3. Experimental procedures

The adhesion ability is the key parameter to the plugging effects. Particles were put into reactor with high-temperature and high-pressure, observing particles packing situation.

Suspension system could carry the particles into reservoir and influence the injectivity of the whole system. HPG and foam were selected.as suspensions. The experimental procedures were as follows: For the HPG suspensions, a) preparing equal volume of suspensions with different solute concentration and same amounts of particles, b) recording respectively the suspended time of particles in each suspension, c) analyzing and comparing the suspension times. For the foam suspensions, a) screening the foam system, b) recording the suspended time. c) Comparing the suspension time.

The above suspension systems were prepared for dynamic plugging experiments. In total, we conducted 19 groups of HPG suspensions and 4 groups of foam suspensions. The experimental procedures were as follows, a) pumping sand-packed pipe vacuum and saturating pipe with formation water; b) measuring the permeability of sand-packed pipe; c) putting the whole instrument into oven with certain temperature; d) injecting the particle system into pipe and recording pressure curves of each pressure tap; e) placing the pipe in oven at constant temperature for 48 h; f) injecting formation water as subsequent water flooding with velocity of 0.5 mL/min, and finally analyzing the pressure curves.

Visual model experiments were designed to observe the migration of particles directly. We made glass sand-pack models and visual microscopic models. The main part of glass sand-pack models were two same pieces of tempered glasses (20 cm long and 15 cm wide), which were bonded by epoxy resin. The quartz sand was filled into interspace between two pieces of glasses, and two-way valves were installed at inlet and outlet. Besides, visual microscopic models were much small (5.0 cm long and 2.0 cm wide), containing one reducing pore, and the width of pore was separately 0.1 mm, 0.3 mm and 0.5 mm.

The procedures of visual experiments were as follows, a) putting all the equipment into oven with 80 ℃, b) saturating the model with formation water and preparing HPG particle system, c) injecting the HPG particle system into model with 200 μL/min, and recording the particle migration.

2.4. Simulation analysis by COMSOL Multiphysics

COMSOL Multiphysics is a general-purpose software platform, based on advanced numerical methods, for modeling and simulating physics-based problems. We simulated and analyzed the particles flowing, as well as the velocity and pressures distribution through the pore. The shape of model in the COMSOL was the same as visual microscopic models. Simultaneously, we derived the force bearing formulas of particles in horizontal and vertical direction. Four situations were simulated including one-flow, two-flow, part-plug, and full-plug. The fluid velocity we set was 1.0 m/s.

3. Results and discussion

3.1. Particle adhesion properties

Fig. 2 shows the shape of particle1-S after adhesion in different temperatures. Once the temperature reached the melting point of coat, the particles in the reactors all got adhered, ranging from 80 ℃ to 140 ℃. Moreover, the degree of adherence increased as temperature increased.

3.2. Suspension system

HPG was the common water-soluble polymer and has been widely applied in the oil and gas industry. Sodium borate, which chemical formula is $Na_2B_4O_7{\cdot}10H_2O$, has broad purposes and low cost.

Fig. 2. Adhesion of plugging particles 1-S in reactor I.

Considering the effects and cost, the first suspension system was compounded by HPG and sodium borate with certain ratios. We measured the suspended time to test the suspension system.

Then we added 0.3% sodium borate into 0.5% HPG suspension to test effects. Within 48 h, the particles kept suspending. The total suspended time was more than 72 h. The suspension ability was excellent.

Excepting HPG system, foam can be used for suspension. Here the foam system is composed of HPG, sodium dodecyl sulfate (SDS) and sodium carboxy methyl cellulose (CMC). Foam composite index F_q is used to characterize foam property, and calculated with the equation below (Zhao et al., 2014):

$$F_q = \int_{t_0}^{t_0+t_{1/2}} f(t)dt \quad (1)$$

where F_q is foam composite index (min·mL); $f(t)$ is foaming volume curves; t_O is time of largest foaming volume (min); $t_{1/2}$ is the half-life time of foam system (min);.

With 0.3 wt% of SDS, and changing the concentration of HPG and CMC, the foaming volume (V), half-life time of foam ($t_{1/2}$) and foam composite index (F_q) were shown in Table 1.

As seen in Table 1, when the concentration of HPG was 0.3%, 0.2% CMC was added, the F_q was largest, which was 54,000, and the foaming power was 600 mL and half-time was 120 min. Therefore, the final formula of foam system was 0.3 wt% SDS + 0.3 wt% HPG + 0.2 wt % CMC. The total suspended time was more than 100 h. The suspension ability was excellent.

3.3. Plugging performance

After testing the adhesion properties and suspension system, we conducted a series of dynamic plugging experiments to confirm particle plugging ability. The experimental parameters were shown in Table 2. Because the wettability of particle coat (modified epoxide resin) and quartz were the same, the permeability might reduce by relatively large margins (Al-Yaseri et al., 2016). If reducing is little in one group of experiment, the particle system might not match with certain parameter.

To evaluate the influence of each parameter on plugging performance, we analyzed separately as follows:

(1) Salinity

We selected models No.9 and No.10 to compare the plugging effects which were influenced by salinity. The salinity of No.9 and No.10 was separately 300 mg/L and 250,000 mg/L, other parameters kept almost the same. The pressure curves in process of particles injection and subsequent water flooding were shown in Fig. 3.

As shown in Fig. 3, during particle injection, the pressure slightly fluctuated at first stage, and when the injection volume reached about 0.6 PV, it began to increase obviously, and the pressure can be up to above 10,000 kPa at 1 PV. During the subsequent water flooding, the pressure can be above 4000 kPa. From the pressure curves of different salinity and the fact of physical plugging and no chemical reactions, the particle system would not be affected by salinity, therefore it would be expected to be adopted in high salinity circumstances, which make the most polymer gel fail.

Table 1
Effect of HPG and CMC concentration on foam properties.

No.	HPG (wt%)	CMC (wt%)	V (mL)	$t_{1/2}$ (min)	F_q (min mL)
1	0.2	0.2	760	60	34,200
2	0.3	0.2	600	120	54,000
3	0.2	0.3	600	70	31,500
4	0.1	0.3	700	20	10,500
5	0.3	0.1	600	110	49,500

Table 2
Parameters of plugging properties of particle system.

No.	PV (mL)	Permeability (10^{-3} μm^2)	Mass fraction of particles (wt%)	Particle type	Injection rate (mL/min)	Salinity (mg/L)
1	200	14,000	8	1-S	1	300
2	199	13,578	8	2-S	1	300
3	205	5571	3	2-S	2	300
4	199	5076	3	2-S	0.5	300
5	200	4540	3	2-S	1	300
6	220	13,908	3	2-S	1	300
7	198	14,489	3	2-S	1	300
8	204	5639	3	2-S	1	300
9	210	8532	5	1-S	2	300
10	179	7961	5	1-S	2	250,000
11	198	13,357	5	1-S	2	250,000
12	207	14,796	1	2-S	1	300
13	213	6230	5	1-S	2	300
14	220	5419	1	1-S	1	300
15	197	5102	2	1-S	1	300
16	81	398	5	1-S	2	300
17	198	2357	5	2-S	2	250,000
18	210	5500	8	2-S	2	250,000
19	191	8615	5	1-S	2	300

(2) Injection rate

Except injection rate, the parameters of the models No.3, No.4 and No.5 were nearly the same. The injection rate of these three experiments were 2 mL/min, 0.5 mL/min, 1 mL/min, their injected system was 5% 1-S particles system and the permeability was all about 5000×10^{-3} μm^2. The pressure curves were shown in below.

From the head faces of models No.3 and No.4, it could be seen that they were blocked completely. Moreover, the residual particles in the container were measured that they were nearly equal to the initial amount. Also it can be seen that from the pressure curves that the inlet pressure increased rapidly and the rest pressures could not be measured. Therefore, the particles actually didn't enter the inside of models and it was meaningless to continue conduct the subsequent water flood, so we didn't perform subsequent operation for models No.3 and No.4. As for model No.5 with injection rate of 1 mL/min, the pressure increased gradually and the particles reached high pressure in the subsequent water flooding, which confirmed that particles could migration along the models and under current parameters 1.0 mL/min was the optimum injection rate. When the injection rate was too high,

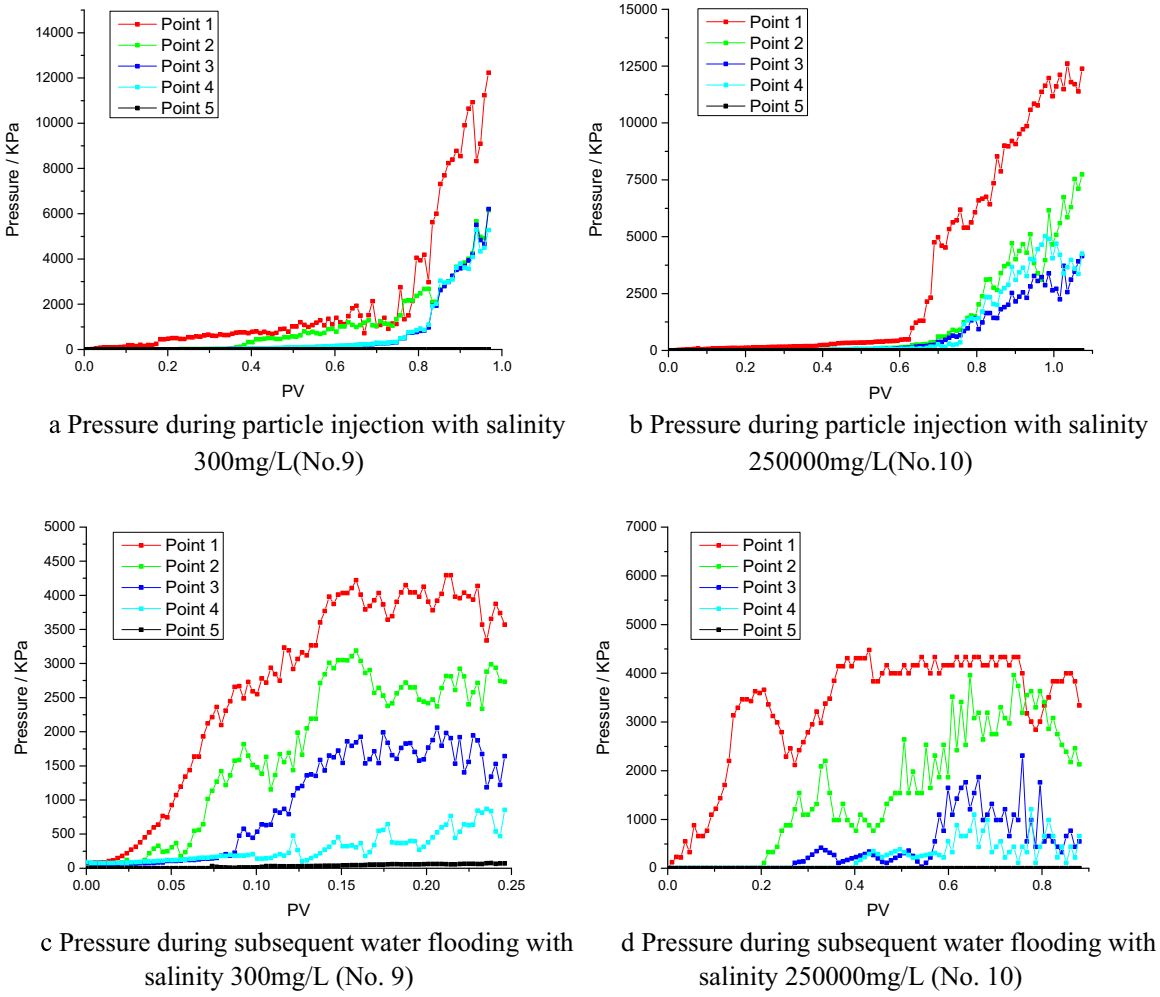

Fig. 3. Pressure curves of particle 1-S in different salinity water. a Pressure during particle injection with salinity 300 mg/L(No.9). b Pressure during particle injection with salinity 250,000 mg/L(No.10). c Pressure during subsequent water flooding with salinity 300 mg/L (No. 9). d Pressure during subsequent water flooding with salinity 250,000 mg/L (No. 10).

the particles would quickly get packed at the inlet and prevent subsequent particle from entering. Furthermore, the pressure could not push the particles into deep, so the particles crowded near the inlet and could not achieve deep migration. On the other hand, when the injection rate was too slow, due to the high temperature, a part of particles had got adhered before entering into pipe and this part of particles had larger diameter, so the pores were plugged by these particles and stopped other particles migration.

(3) Permeability

Models No.10 and No.11, No.7 and No.8 were selected to compare their plugging effects due to the difference in permeability. The permeability of No.8 and No.7 was 5639×10^{-3} μm^2 and $14{,}489\times10^{-3}$ μm^2, 3% particle 2-S was injected and injection rate was 1.0 mL/min (Fig. 4). The subsequent water flooding pressure curves of No.8 and No.7 were shown in Fig. 5.

From the curves, the breakthrough pressure was separately 9812 kPa and 5355 kPa, so effective plugging was formed in both models, and the effect in lower permeability model No.8 was better than in high permeability model No.7.

In addition, 5% particle 1-S was injected into model with the permeability 5437×10^{-3} μm^2, the pressure during subsequent water flooding was shown in Fig. 6. It showed that the maximum pressure was only about 440 kPa, so the plugging effect was rather not satisfactory. Considering the diameters and coat, all the phenomena confirmed that there was an optimal matching relation between particle and permeability.

(4) Mass Fraction

Different concentration 8%, 3% and 1% of particle 2-S was injected into models No.6, No.2 and No.12 with permeability about $14{,}000\times10^{-3}$ μm^2, and the injection rate was 1.0 mL/min. The pressure during subsequent water flooding was shown in Fig. 7.

Fig. 7 illustrated when the mass fraction was 1% and 8%, models No.6 and No.12 didn't achieve the effective plugging, and with breakthrough pressures were only 1190 kPa and 6.0 kPa. In contrast, the pressure curve of model No.2 with concentration of 3% showed that the plugging was successful and its breakthrough pressure was about 17,221 kPa (Fig. 8). The mass fraction of particle 2-S could be 3% for the permeability about $14{,}000\times10^{-3}$ μm^2.

Similar to the 2-S particle, different concentration 5%, 1% and 2% of particle 1-S was injected into models No.13, No.14 and No.15 with permeability about 5000×10^{-3} μm^2. Only model No.15 acquired relatively high breakthrough pressure of 4218.42 kPa, so the optimum mass fraction of particle 1-S was 2% in the permeability of 5000×10^{-3} μm^2.

Generally speaking, the low mass fraction would not achieve effective plugging because of the low injection volume. And the high mass fraction might have negative impact on the injectivity of system. Therefore, mass fraction was also an important factor in the particles

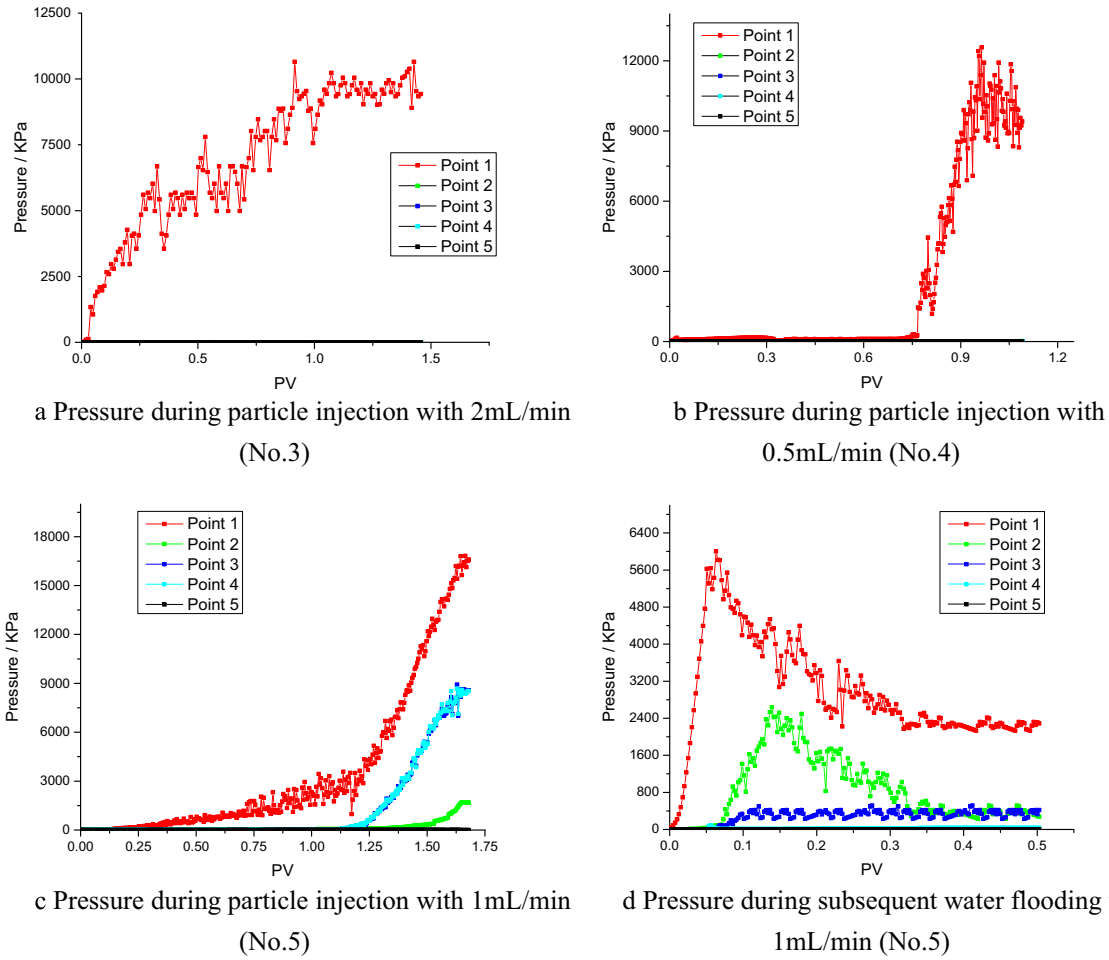

a Pressure during particle injection with 2mL/min (No.3)

b Pressure during particle injection with 0.5mL/min (No.4)

c Pressure during particle injection with 1mL/min (No.5)

d Pressure during subsequent water flooding with 1mL/min (No.5)

Fig. 4. Pressure curves of particle 2-S with different injection rate. a Pressure during particle injection with 2 mL/min (No.3). b Pressure during particle injection with 0.5 mL/min (No.4). c Pressure during particle injection with 1 mL/min (No.5). d Pressure during subsequent water flooding with 1 mL/min (No.5).

system operations. Al-Yaseri et al. (2015) confirmed that higher fines concentrations led to greater reduction in porosity and permeability. However, combining with the properties of particle itself, the higher mass fraction was not always better, but for the mediate amount.

3.4. Visual experiments

(1) Glass sand-pack models

The glass sand-pack models were shown in Fig. 9. The mass fraction of HPG particle 2-S (74 μm) system was selected as 5% and the quartz

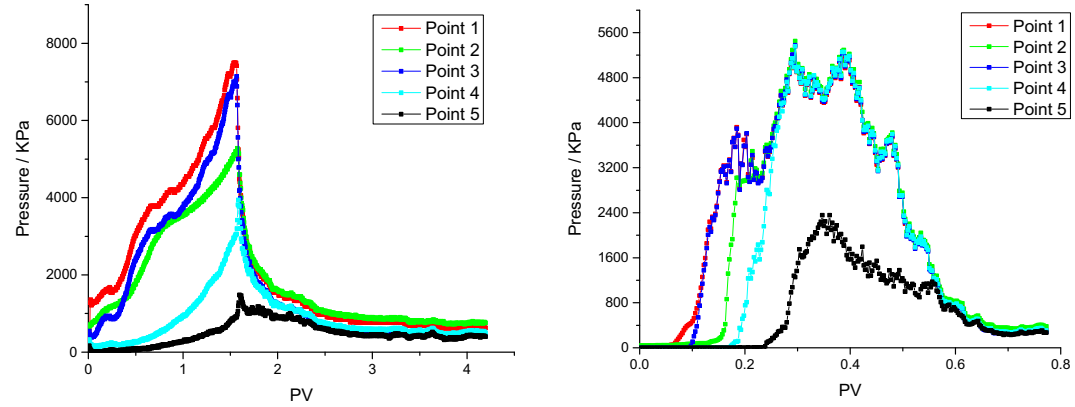

a Pressure during subsequent water flooding with permeability about $5000\times10^{-3}\mu m^2$ (No.8)

b Pressure during subsequent water flooding with permeability about $15000\times10^{-3}\mu m^2$ (No.7)

Fig. 5. Pressure curves of particles 2-S with different permeability. a Pressure during subsequent water flooding with permeability about 5000×10^{-3} μm^2 (No.8). b Pressure during subsequent water flooding with permeability about $15{,}000\times10^{-3}$ μm^2 (No.7).

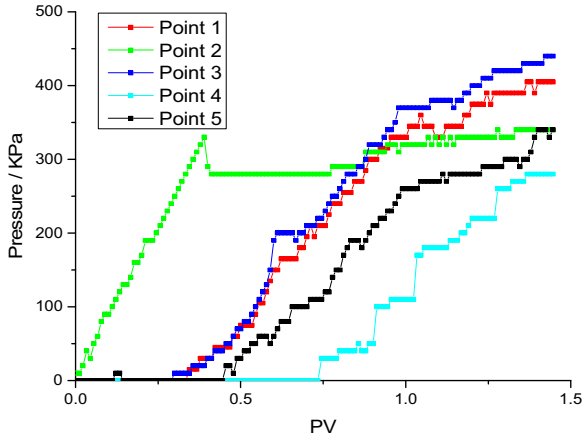

Fig. 6. Pressure during subsequent water flooding with permeability about 5000×10^{-3} μm^2 after particles 1-S injection (No.10).

sand filled into models were selected as 10, 20, 40 and 50 mesh.

When the mesh of quartz sand was 10 (Fig. 10a), particles transported smoothly and achieved the goal of deep migration and avoiding plugging in advance. Particles gradually covered increasing areas of model, and we could clearly observe the migration trends after 45 min. The phenomenon was accordance with former dynamic plugging performance, and high permeability could improve the plugging performance. When eliminating the obstacle of injectivity, plugging particles would be one of the best plugging agents.

When the mesh of quartz sand was 20 (Fig. 10b), more particles concentrated at the inlet. Based on Fig. 10b, at the initial state the particles were evenly distributed in every direction, keeping the state of single particle. When the injection continued (15 min), a part of particles began to adhere and plug the pore. In this situation, the subsequent particles would be harder to transport into deep, with the push from system, only small amounts of particles would achieve this. The number of such particle was less than particles in the 10 mesh model. As more particles were injected, a majority of them packed at the inlet. If the part plugging was formed, the speed of subsequent plugging forming would be much faster. We observed particles at this state had migrated circularly. Therefore, the plugging was nearly formed and continued injection would be ineffective.

When the mesh of quartz sand was 40 (Fig. 10c), the packs at the inlet were larger and the particles transported into deep were less during the same migration time (15 min). Besides, the packs would have impact on the origin structure of quartz sand. With the injection continued, we could observe the particles focused quartz sand to move. Therefore, it was confirmed that the particle system would influence the structure of reservoir mineral, and the reason was the driving force from the particles and the high viscosity system itself. And this should be considered during the field operation, especially for the velocity sensitivity mineral such as kaolinite. Besides, the location of particles

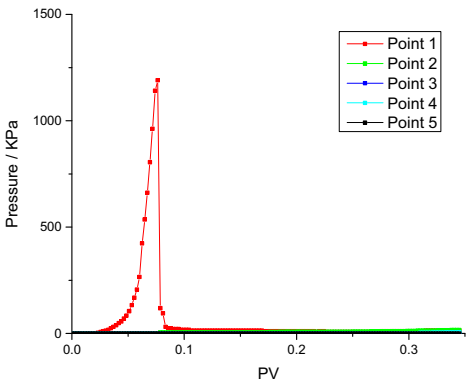

a Pressure during subsequent water flooding with mass fraction of 8% (No.6)

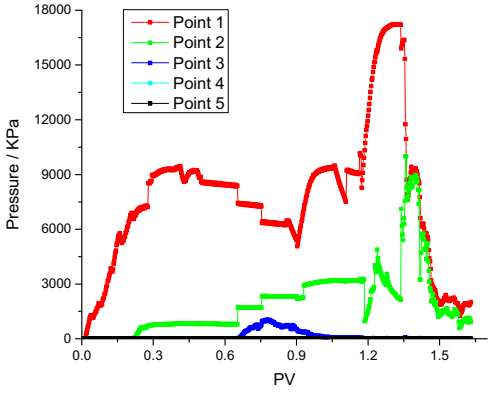

b Pressure during subsequent water flooding with mass fraction of 3% (No.2)

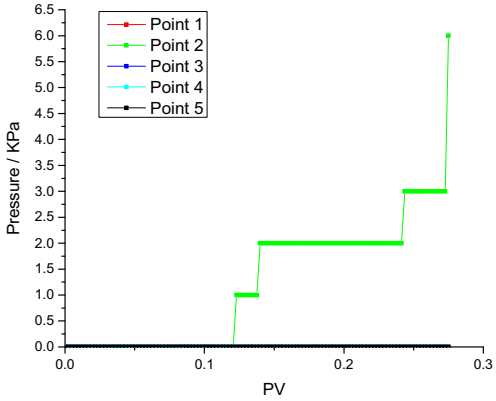

c Pressure during subsequent water flooding with mass fraction of 1% (No.12)

Fig. 7. Pressure curves of particles 2-S with different mass fraction. a Pressure during subsequent water flooding with mass fraction of 8% (No.6). b Pressure during subsequent water flooding with mass fraction of 3% (No.2). c Pressure during subsequent water flooding with mass fraction of 1% (No.12).

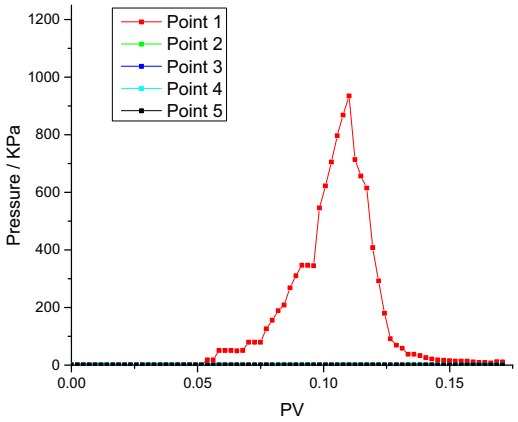

a Pressure during subsequent water flooding with mass fraction of 5% (No.13)

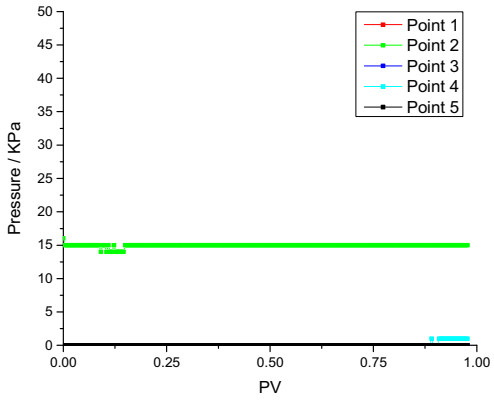

b Pressure during subsequent water flooding with mass fraction of 1% (No.14)

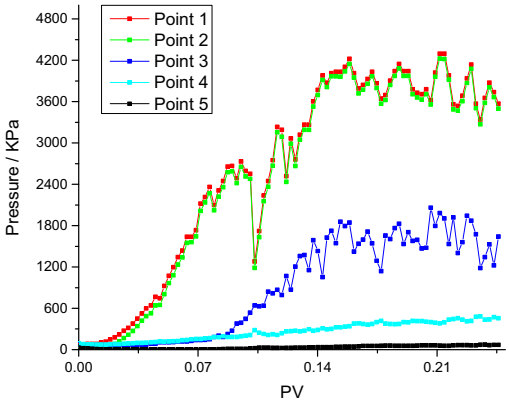

c Pressure during subsequent water flooding with mass fraction of 2% (No.15)

Fig. 8. Pressure curves of particles 1-S with different mass fraction. a Pressure during subsequent water flooding with mass fraction of 5% (No.13). b Pressure during subsequent water flooding with mass fraction of 1% (No.14). c Pressure during subsequent water flooding with mass fraction of 2% (No.15).

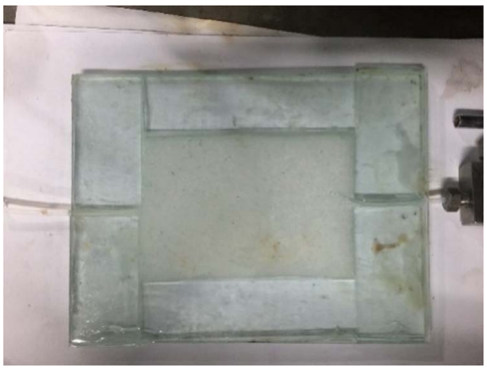

Fig. 9. Glass sand-packing model.

packed was more focused near the inlet. The packed area, which was more clearly than 10 mesh and 20 mesh experiments, almost didn't change since 15 min. This suggested that the plugging ability of HPG particle system would decrease under low permeability environment and real effects scope would get closer to the near-wellbore area. So the selection of particle system should be considered carefully about permeability.

When the mesh of quartz sand was 50 (Fig. 10d), the injectivity of HPG particle system decreased obviously, and the particles packed in the rubber hose and only several particles transported into deep, most particles stayed at the inlet area only after 15 min. As shown in Fig. 10d, from the 15 to 45 min the pack in the rubber hose gradually increased and the distribution of particles didn't change since 15 min. So the plugging was completed around 15 min and subsequent flooding were all ineffective.

In conclusion, the visual experimental results confirmed that there was a moderate and matched pore size for the HPG particle system.

(2) Visual microscopic models

For the visual microscopic models, we conducted four groups of experiments. Except injection rate, other parameters kept all the same. To be convenient to observe single particle migration, the mass fraction was 0.2%. Injection rate for four groups was set respectively 200 μL/min, 150 μL/min, 100 μL/min and 50 μL/min.

- No.1 (200 μL/min)

In model No.1, the first stopped particles appeared only after injection started about 22 s (Fig. 11a). However, with the flow of system, this particle was pushed away by the subsequent particle, until in 59 s, the next stopped particle appeared. The packing was started

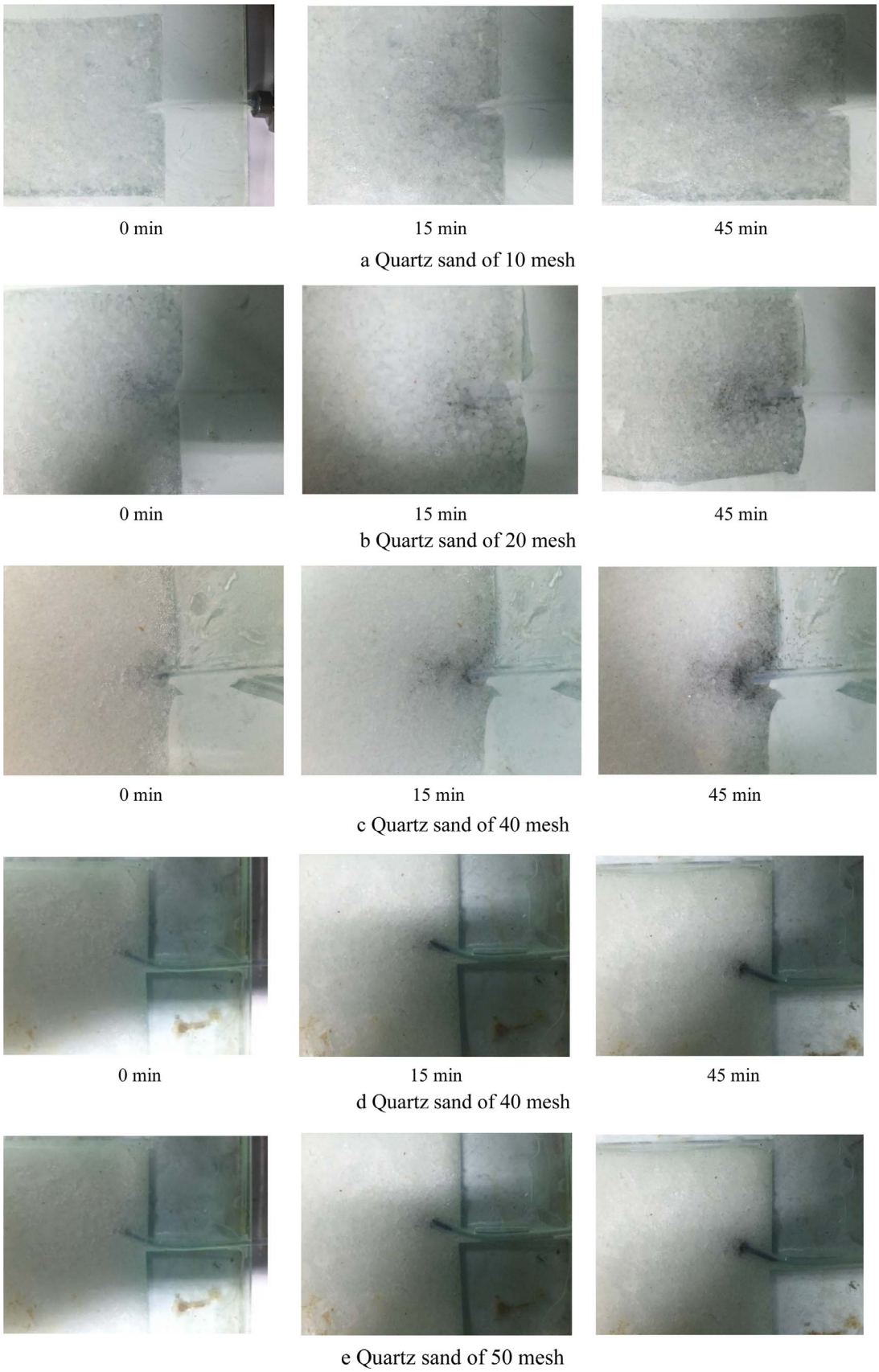

Fig. 10. Dynamic migration of particles in glass model of quartz sand with different size. a Quartz sand of 10 mesh. b Quartz sand of 20 mesh. c Quartz sand of 40 mesh. d Quartz sand of 40 mesh. e Quartz sand of 50 mesh.

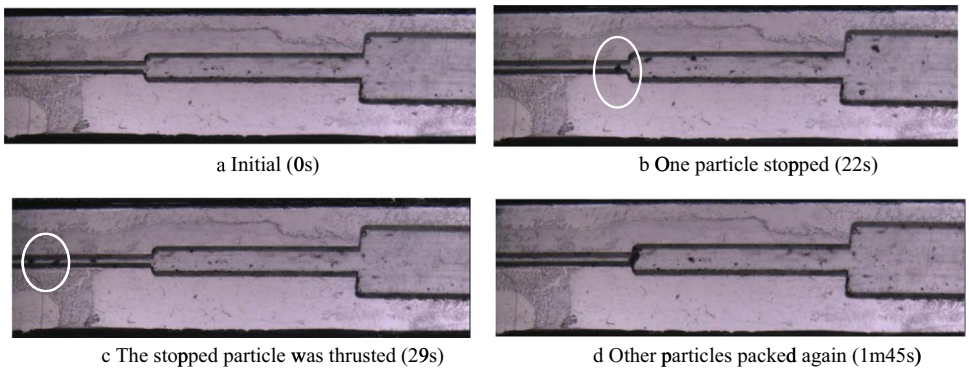

Fig. 11. Plugging in visual microscopic model No.1. a Initial (0 s). b One particle stopped (22 s). c The stopped particle was thrusted (29 s). d Other particles packed again (1 m45 s).

about 1 m 45 s. The situation illustrated that the packing was not once shaped when the diameter of particle was smaller than pore. At the initial state, when the amount of particle was small, the packing was difficult to form and the stopped particle might be pushed by the subsequent particle.

- No.2 (150 μL/min)

The first stopped particle in model No.2 appeared in 3 m 24 s. After 9–3 m 33 s, there had been four particles which were stopped. And when the time to 3 m 41 s, the packing became faster and nearly completed at 3 m 57 s. It suggested that the process of packing was accelerated. Comparing with model No.1, when the injection rate got slower, the possibility of being pushed was decreased, so we didn't observe the situation of push-away happened in model No.2. For the single particle, the difficulty level of packing didn't change, which was still related to diameter and amounts, etc.

The accelerated packing process was also confirmed that several situations happened in dynamic plugging experiments, such as accelerated increasing of pressure. When the amounts of particles were small, the changing rate of injection pressure was low. However, when the amounts had accumulated to a certain degree, the packing began to accelerate, as well as the changing rate of injection pressure.

- No.3 (100 μL/min)

The injection rate of model No.3 was 100 μL/min, the rate got further reduced and the time of forming packing was longer than model No.2. The whole situation was nearly the same with model No.2.

- No.4 (50 μL/min)

For model No.4, in the first 7 m 46 s it repeated the situation of former three groups. But at 7 m 50 s, the packing, which had been formed, was pushed away by one single particle and had to be formed again. Although the packing was much larger than single particle, but due to the instability of the structure, when crashed with subsequent particle, it was possible to be pushed away, the whole packing would increase again until steady.

The time of packing was longer than the former three groups and the packing was ever pushed away, so if we expected that particle could express plugging effects, their injection volume should be large enough. The insufficiency of injection volume might lead packing to be pushed and this would be negative to the whole plugging.

3.5. Simulation

The model we designed was the same with visual microscopic model, and the structure was shown as Fig. 15.

The system transported from inlet to outlet with a certain speed of V. When the particle entered the narrow pore from wide pore, due to the mass and momentum conservation, the transport speed in the narrow pore must be improved. If the total diameter of particles after adhesion was larger than the width of narrow pore, the plugging would happen. In the whole simulation, the deformation of particles would not be considered.

The stress state of particle would directly influence the particle migration process. Therefore, we selected four specific situations to analyst the stress state of particle in each case: one single particle migration (one-flow), two adherent particles migration (two-flow), two adherent particles plugging partly (part-plug) and two adherent particles plugging fully (full-plug).

In order to simulate the force, we should derivate the formula of the force firstly. And the force on the particle could be described as

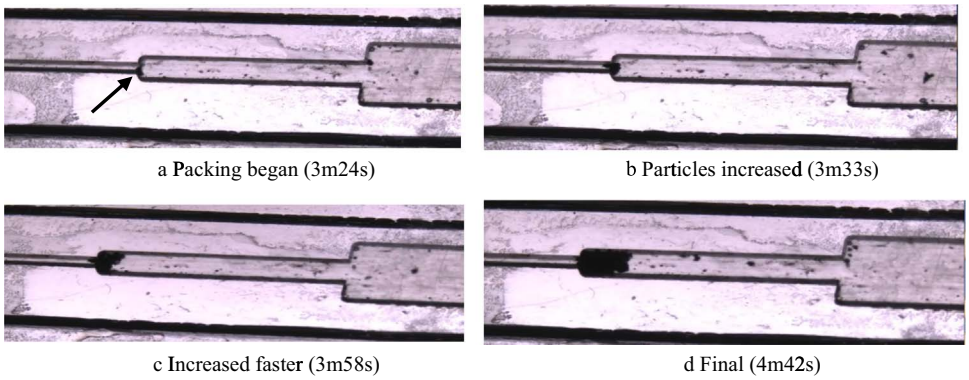

Fig. 12. Plugging in visual microscopic models No.2. a Packing began (3 m24 s). b Particles increased (3 m33 s). c Increased faster (3 m58 s). d Final (4 m42 s).

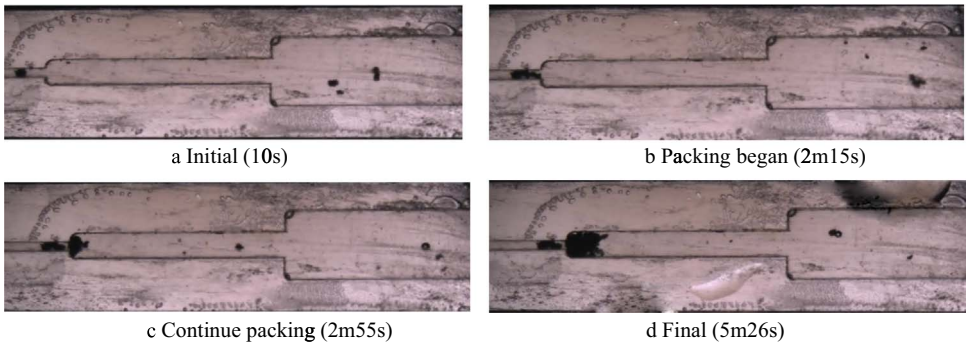

Fig. 13. Plugging in visual microscopic model No.3. a Initial (10 s). b Packing began (2 m15 s). c Continue packing (2 m55 s). d Final (5 m26 s).

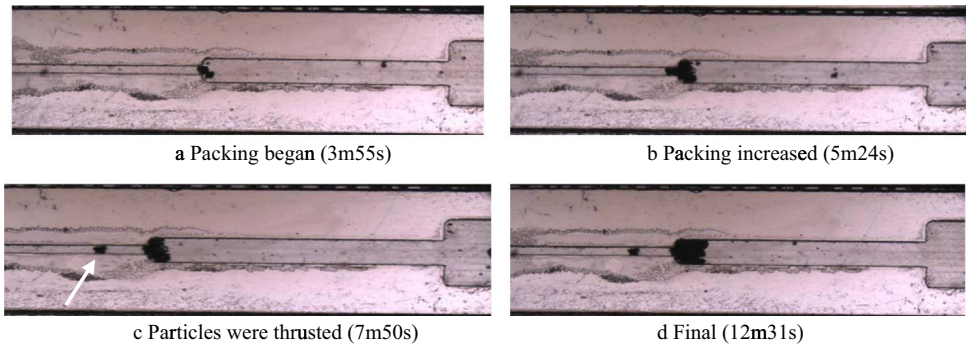

Fig. 14. Plugging in visual microscopic model No.4. a Packing began (3 m55 s). b Packing increased (5 m24 s). c Particles were thrusted (7 m50 s). d Final (12 m31 s).

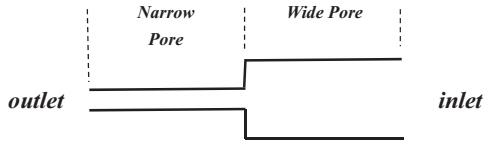

Fig. 15. Structure of bidimensional pore.

$$\vec{F} = F_x \bullet \vec{i} + F_y \bullet \vec{j} \tag{2}$$

where F_x and F_y are the components of $\vec{F}$ in x and y axis direction.

And the force from the wall of particle to the fluid is calculated as

$$\vec{F_H} = \int T^H \bullet \vec{n} \bullet d\Gamma \tag{3}$$

where T^H is the tensor of hydraulic, the $\vec{n}$ and T^H are calculated as follows:

$$\vec{n} = (n_x \bullet \vec{i} + n_y \bullet \vec{j}) = \begin{bmatrix} n_x \\ n_y \end{bmatrix} \tag{4}$$

$$T^H = -P \bullet I + \mu(\nabla u + \nabla u^T) \tag{5}$$

where

$$I = \begin{bmatrix} 1 & 0 \\ 0 & 1 \end{bmatrix} \tag{6}$$

$$\nabla = \begin{pmatrix} \frac{\partial}{\partial x} \\ \frac{\partial}{\partial y} \end{pmatrix} \tag{7}$$

$$\vec{u} = (u, v) \tag{8}$$

where u and v are the components of $\vec{u}$ in X and Y Axis direction. Based on *Newton's Third Law*, due to the $\vec{F_H}$ is from particle to the fluid, so

$$\vec{F} = -\vec{F_H} \tag{9}$$

Substituting Eq. (5) into Eq. (3), one can re-write Eq. (3) as follows:

$$\vec{F_H} = \int [-P \bullet I + \mu(\nabla u + \nabla u^T)] \bullet \vec{n} \bullet d\Gamma \tag{10}$$

And the ∇u could be described as

$$\nabla u = \begin{pmatrix} \frac{\partial}{\partial x} \\ \frac{\partial}{\partial y} \end{pmatrix} \bullet (u, v) \tag{11}$$

One can re-write Eq. (11) as

Table 3
Stress state of one particle migration.

No.	1	2	3	4	5	6	7	8
Time (s)	0	1.00E−04	2.00E−04	3.00E−04	4.00E−04	5.00E−04	6.00E−04	7.00E−04
F_x (N/m)	−392.46	5.43E−08	4.58E−10	5.84E−11	1.01E−11	1.66E−11	1.48E−12	−2.58E−12
F_y (N/m)	−0.00493	7.23E−12	3.48E−13	1.24E−13	1.88E−13	−5.33E−14	6.75E−14	6.04E−14

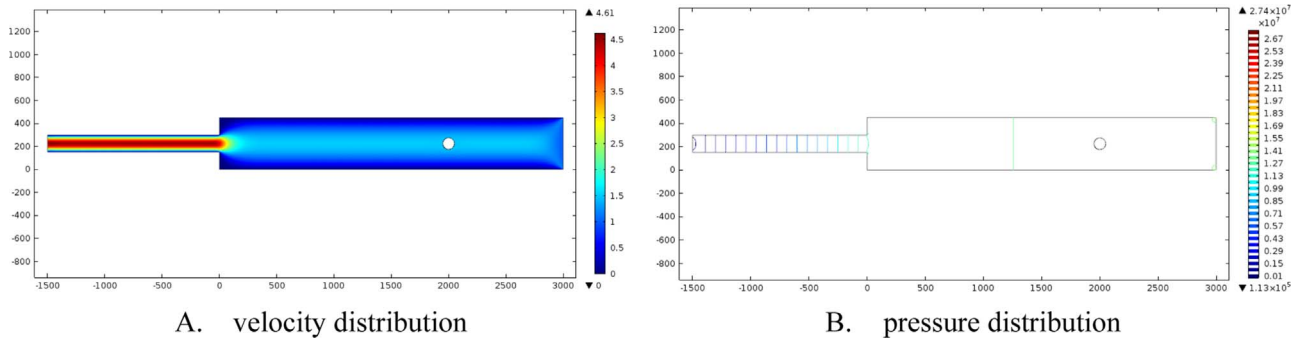

Fig. 16. Distribution of one single particle along migration. a velocity distribution. b pressure distribution.

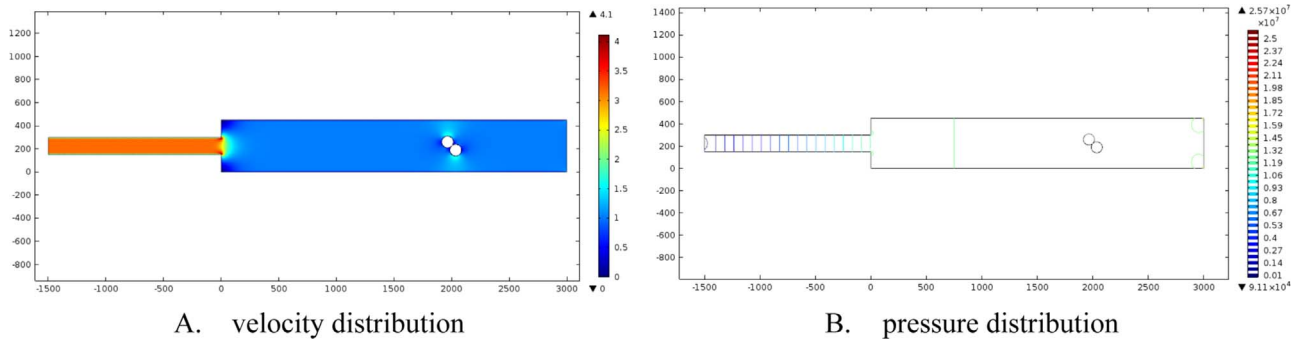

Fig. 17. Distribution of two adherent particle along migration. A velocity distribution. B pressure distribution.

Table 4
Stress state of two adherent particles migration.

No.	1	2	3	4	5	6	7	8
Time (s)	0	1.00E−04	2.00E−04	3.00E−04	4.00E−04	5.00E−04	6.00E−04	7.00E−04
F_x (N/m)	−659.55	−1.55E−08	6.28E−10	1.69E−09	2.26E−09	2.21E−09	9.31E−10	1.35E−09
F_y (N/m)	24.172	8.00E−08	9.11E−10	−1.94E−10	−6.23E−10	−6.19E−10	−2.59E−10	−3.76E−10

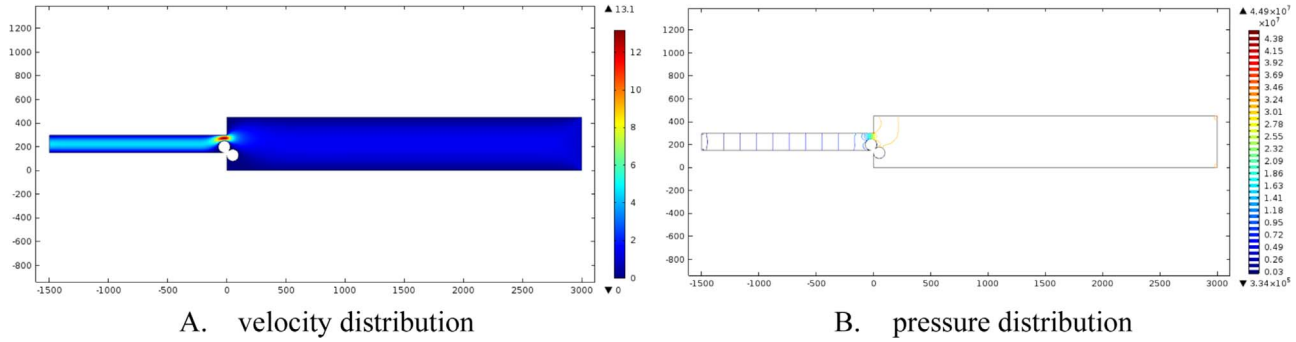

Fig. 18. Distribution of two adherent particle plugging partly. A velocity distribution. B pressure distribution.

$$\nabla \boldsymbol{u} = \begin{bmatrix} \frac{\partial u}{\partial x} & \frac{\partial v}{\partial x} \\ \frac{\partial u}{\partial y} & \frac{\partial v}{\partial y} \end{bmatrix} = \begin{bmatrix} u_x & v_x \\ u_y & v_y \end{bmatrix} \tag{12}$$

So it can obtain

$$\boldsymbol{\mu}(\nabla \boldsymbol{u} + \nabla \boldsymbol{u}^T) = \boldsymbol{\mu} \begin{pmatrix} 2u_x & v_x + u_y \\ u_y + v_x & 2v_y \end{pmatrix} \tag{13}$$

and

$$\boldsymbol{\mu} \begin{pmatrix} 2u_x & v_x + u_y \\ u_y + v_x & 2v_y \end{pmatrix} \bullet \begin{bmatrix} n_x \\ n_y \end{bmatrix} = \begin{bmatrix} \mu[2u_x \bullet n_x + (v_x + u_y) \bullet n_y] \\ \mu[2u_y \bullet n_y + (v_x + u_y) \bullet n_x] \end{bmatrix} \tag{14}$$

Besides, the $-\mathrm{P} \bullet \mathbf{I} \bullet \vec{n}$ can be expressed as

$$-\mathrm{P} \bullet \mathbf{I} \bullet \vec{n} = -\mathrm{P} \bullet \begin{bmatrix} 1 & 0 \\ 0 & 1 \end{bmatrix} \bullet \begin{bmatrix} n_x \\ n_y \end{bmatrix} = \begin{bmatrix} -Pn_x \\ -Pn_y \end{bmatrix} \tag{15}$$

Therefore, $\vec{F}$ can be obtained by Eqs. (14) and (15). In COMSOL, the variables, *spf. T_stressx* and *spf. T_stressy*, were the components of T_H in X and Y Axis direction, so we could calculate the value of $\vec{F}$.

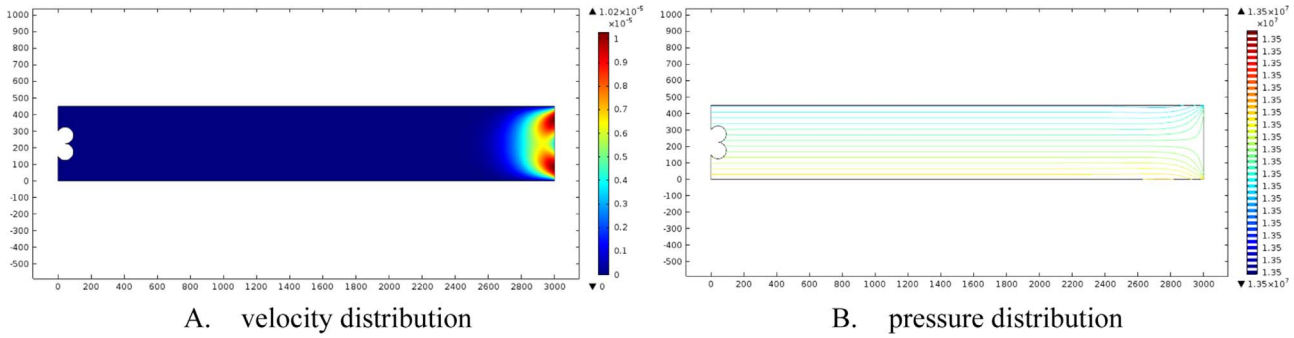

Fig. 19. Distribution of two adherent particle plugging fully. A velocity distribution. B pressure distribution.

Table 5
Stress state of two adherent particles plugging partly.

F_x (N/m)	F_y (N/m)
−2961.2	−761.36

Table 6
Stress state of two adherent particles plugging fully.

F_x (N/m)	F_y (N/m)
−2018.4	1.5591E−4

(1) One-flow

When the one single particle migration was simulated, the particle was in equilibrium and didn't get acceleration under the steady flow velocity. Only the particle and system existed relative speed, the particle would be acted upon the force. Therefore, we assumed that the pure system flow with steady velocity and one single particle, which initial velocity was zero, was thrown into fluid. In this situation, the force was applied on this single particle (Table 3).

As shown in Fig. 16a, the flow fluid was symmetrical and the velocity of narrow pore was much faster than wide narrow. The closer to the wall, the flow velocity slower and the velocity at the wall was zero.

When the fluid velocity was 1.0 m/s, on the X axis direction, the force which was applied on particle was 392.46 N at time zero. After 0.0002 s, this force decreased to 4.58×10^{-10} N. And the force on the Y axis direction could be ignored. In a very short time (0.0015 s) the particle could be in equilibrium. Then the particle flowed in the fluid with same velocity.

Therefore, when one single particle migrated, the direction would be the same with fluid. So keeping the particle single during the migration would help the particle to transport to the certain direction. Due to the large pore path, the fluid would prefer to enter into these path. During this process, the fluid would bring the single particle to destination pore and plug them.

(2) Two-flow

The situation of two-flow was similar to the one-flow, however, because of the difference in shape, the magnitude and direction of the force should also be different.

According to Fig. 17 and Table 4, the flow field changed slightly, comparing with one single particle. Due the shape of adherent particle, the flow fluid around the particles would change obviously. When the velocity was 1.0 m/s, the force on the X axis direction which was applied on particle was 659.55 N at time zero. After 0.0002 s, this force decreased to 6.28×10^{-10} N. And the force on the Y axis direction was 24.172 N and decreased to 9.11×10^{-10} N after 0.0002 s. Therefore, there was a slight side velocity on the particles.

Although the changing was very quick, there was still a side velocity on the adherent particles and this velocity might lead the particle to contact the pore wall in advance, weakening the plugging effects. So keeping the particles single during the transportation should be attached the importance.

(3) Part-plug

In this situation, the adherent particles stayed at the pore, the flow fluid would keep up the pressure to the particles. In this case, the fluid could be regarded as incompressible fluid (Fig. 18 and 19 and Tables 5 and 6).

Different with state of flow, the force applied to particles in this case was much larger. When the particle stayed at the pore, the force on the X and Y axis direction was separately 2961.2 N and 761.36 N. This force was much larger than the force which needed to start flow. Therefore, the material strength should be considered carefully. The force could also explain the situation of push-away happened in Visual Microscopic Models, the force applied on the particles suddenly increased and made the particle unsteady, increasing the possibility to be pushed away.

(4) Full-plug

When the pore was plugged completely, the velocity of flow fluid was nearly zero. the force on the X axis direction which was applied on particle was 2018.4 N and the force on the Y axis direction could be ignored. It was worth mentioning that force in X direction was less than the force of part-plug. When the channel got narrower, the pressure would be increased in response. Therefore, the unsteady structure of packing would be aggravated during the part-plug period, when the pore was plugged fully, the pressure decreased instead.

4. Conclusion

(1) The diameter of particle ranged from 40 μm to 200 μm and the particles could keep packing under high temperature and high pressure conditions. The HPG and foam system could act as suspension system.
(2) The developed particles with core and coat may be successfully used in high temperature(140 °C) and high salinity(250,000 mg/L) environment, which provides a possible solution for the challenging situation.
(3) Combined lab core experiments with visual model experiments,

COMSOL Multiphysics software platform can be used to investigate and analyze the flow line and stress state, which provides a useful tool for study the microscopic action and state.

Acknowledgement

The authors thank the National Natural Science Foundation of China (No. 51174216) and State Key Science & Technology Project of China (Nos. 2011ZX05009-004, and 2011ZX05052) for their financial support to carry out this research. The insightful and constructive comments of the anonymous reviewers are also gratefully acknowledged.

References

Abrams, Albert, 1977. Mud design to minimize rock impairment due to particle invasion. J. Pet. Technol. 29 (05), 586–592.
Ahmed, Al-Yaseri, et al., 2016. Impact of fines and rock wettability on reservoir formation damage. Geophys. Prospect. 64 (4), 860–874.
Al-Yaseri, Ahmed Z., et al., 2015. Pore-scale analysis of formation damage in Bentheimer sandstone with in-situ NMR and micro-computed tomography experiments. J. Pet. Sci. Eng. 129, 48–57.
Bai, Baojun, Zhang, Hao, 2011. Preformed-particle-gel transport through open fractures and its effect on water flow. SPE J. 16 (02), 388–400.
Bai, Baojun, 2003. The basic research of the deep profile control and oil displacement of Pre-gel Particles. China University of Geoscience (Beijing), Beijing.
Bryant, Steven L., Rabaioli, M.R., Lockhart, Thomas P., 1996. Influence of syneresis on permeability reduction by polymer gels. SPE Prod. Facil. 11 (04), 209–215.
Civan, F., 2007. Reservoir Formation Damage Fundamentals, ModelingAssessment and Mitigation second ed. Gulf Publishing Company, Houston, USA, 1114.
Civan, Faruk, Vinh, Nguyen, 2005. Modeling particle migration and deposition in porous media by parallel pathways with exchange. Chapter 11, 457-484.
Cui, Xiaohong, et al. 2011. A novel PPG enhanced surfactant-polymer system for EOR. SPE Enhanced Oil Recovery Conference. Society of Petroleum Engineers.
Elsharafi, Mahmoud, Baojun Bai, 2015. Minimizing formation damage for preformed particle gels in Mature Reservoirs. SPE Asia Pacific Enhanced Oil Recovery Conference. Society of Petroleum Engineers.
Fragachan, F.E., et al. 1996. Controlling water production in naturally fractured reservoirs with inorganic gel. International Petroleum Conference and Exhibition of Mexico. Society of Petroleum Engineers.
Galindo, Kay A. et al. 2015. High Temperature, High performance water-based drilling fluid for extreme high temperature wells. SPE International Symposium on Oilfield Chemistry. Society of Petroleum Engineers.
Hernando, L., et al. 2016. Polymer-enhanced foams for water profile control. SPE Improved Oil Recovery Conference. Society of Petroleum Engineers.
Hild, G.P., Wackowski, R.K., 1999. Reservoir polymer gel treatments to improve miscible CO_2 flood. SPE Reserv. Eval. Eng. 2 (02), 196–204.
Zhao, Jiangyu, Pu, Wanfen, Li, Yibo, et al., 2014. Laboratory selection and performance evaluation on high temperature and high salinity resistant foam system. Oilfield Chem. 32 (4), 65–69.
Jones, P.W., Baker, R.O., 1992. Profile control in Virginia Hills EOR injectors. SPE/DOE Enhanced Oil Recovery Symposium. Society of Petroleum Engineers.
Khatib, Z.I., Vitthal, Sanjan, 1991. The use of the effective-mediumtheory and a 3D network model to predict matrix damage in sandstone formations. SPE Prod. Eng. 6 (02), 233–239.
Lakatos, I., et al. 1996. A novel well treatment method based on in-situ hydrolysis and flocculation of inorganic compounds. SPE/DOE Improved Oil Recovery Symposium. Society of Petroleum Engineers.
Zheng, Lihui, Zhang, Mingwei, 2012. Review of basic theory for lost circulation control. Oil Drill. Prod. Technol. 34 (05), 1–9.
Liu, He, et al., 2006. Granular-polymer-gel treatment successful in the Daqing Oilfield. SPE Prod. Oper. 21 (01), 142–145.
Ojukwu, Kelechi Isaac, et al., 2005. Life-cycle profile control in subhydrostatic wells of South Oman. SPE Annual Technical Conference and Exhibition. Society of Petroleum Engineers.
Li, Qi, Guo, Jianming, Wang, Kuisheng, 1995. Quantitative design method for shielding temporary plugging. Drill. Fluid Complet. Fluid 12 (05), 36–38.
Quadri, Syed Mohamid Raza, et al., 2015. Application of biopolymer to improve oil recovery in high temperature high salinity carbonate reservoirs. Abu Dhabi International Petroleum Exhibition and Conference. Society of Petroleum Engineers.
Sharma, Gaurav, Mohanty, Kishore, 2013. Wettability alteration in high-temperature and high-salinity carbonate reservoirs. SPE J. 18 (04), 646–655.
Tran, Tung Vu, Faruk, Civan, Ian D., Robb., 2010. Effect of permeability impairment by suspended particles on invasion of drilling fluids. IADC/SPE Asia Pacific Drilling Technology Conference and Exhibition. Society of Petroleum Engineers.
Tran, Tung V., Civan, Faruk, Robb, Ian D., 2009. Correlating flowing time and condition for perforation plugging by suspended particles. SPE Drill. Complet. 24 (03), 398–403.
Luo, Xiangdong, Luo, Pingya, 1992. The applied research of shielding temporary plugging technique in reservoir protection. Drill. Fluid Complet. Fluid 9 (2), 19–27.
Xiong Chunming, et al., 2007. Technologies of water shut-off and profile control: an overview. Pet. Explor. Dev. 34 (1), 83–88.
Zhao, H., et al. 2005. Field pilots of microbial flooding in high-temperature and high-salt reservoirs. SPE Annual Technical Conference and Exhibition. Society of Petroleum Engineers.
Zhao Xiutai, et al., 2015. The current research situation and development trend of particle profile-control plugging agents. Oil Drill. Prod. Technol. 37 (4), 105–112.